Radio Science, Volume 32, Number 3, Pages 1149–1160, May–June 1997

First observations of Kelvin-Helmholtz billows in an upper level jet stream using VHF frequency domain interferometry

Phillip B. Chilson[1]
Max-Planck-Institut für Aeronomie, Katlenburg-Lindau, Germany

Andreas Muschinski
Institut für Meteorologie und Klimatologie der Universität Hannover, Hanover, Germany

Gerhard Schmidt
Max-Planck-Institut für Aeronomie, Katlenburg-Lindau, Germany

Abstract. In this paper we report the first high-resolution observations of upper tropospheric Kelvin-Helmholtz billows using VHF frequency domain interferometry (FDI). The measurements were made using the sounding system VHF radar located in the German Harz Mountains operating at the frequencies of 53.25 and 53.75 MHz. Through an application of the FDI technique it has been possible to track the altitude of thin scattering layers with an accuracy of a few tens of meters and a temporal resolution of 13 s. Taking advantage of the FDI technique, we found several examples of Kelvin-Helmholtz instability (KHI) in regions coinciding with large values of wind shear. One particularly good example is presented in detail. The KHI occurred just below the axis of the jet at an altitude of 9.1 km. It produced oscillations in the vertical velocity field in the altitude range of 8–10 km. The oscillations had a local period of 90 s and persisted over a time interval of 10 min. On the basis of the magnitude of the horizontal wind at the time and height of the KHI, the billow train had a horizontal extent of about 27 km, while the horizontal length of the individual billow amounted to about 4.0 km. The 90-s oscillations were also observed in the radar signal power, the FDI-derived layer height, and the coherence between the received radar signals for the two frequencies. Using the FDI data, we were able to identify the individual billows located within the train and observe their maximum crest-to-trough amplitudes to be between 220 and 230 m. This was less than the conventional radar resolution of 300 m used during the experiment.

Introduction

Radars have played an important role in the study of Kelvin-Helmholtz instability (KHI) in the free atmosphere and its association with clear-air turbulence (CAT) [*Gossard and Hooke*, 1975; *Fritts and Rastogi*, 1985; *Gage*, 1990; *Gossard*, 1990]. Since the first studies of clear-air turbulence by radar in the late 1960s and early 1970s, a close connection between CAT and the characteristic billow structures of KHI has been directly observed [*Hicks and Angell*, 1968; *Atlas et al.*, 1970; *Browning and Watkins*, 1970; *Browning*, 1971; *Reed and Hardy*, 1972]. Basically, KHI is a dynamic instability that forms in strongly sheared and statically stable flows. Consequently, the occurrence of KHI is associated with small Richardson numbers Ri. On the grounds of theoretical considerations, a necessary but not sufficient condition for the production of KHI is that $Ri \leq 0.25$. *Browning* [1971, p. 297] studied 17 individual cases of Kelvin-Helmholtz billows and found that "Apart from events associated with shear zones of very small scale, the Ri fell within the range 0.15–0.3, broadly consistent with the theoretically predicted $Ri_c = 0.25$."

KHI structures come in a variety of shapes, depending on the environmental conditions and the stage of their development. On the basis of high-resolution radar observations, *Browning and Watkins* [1970] characterized the structures that they detected as single layers, breaking waves, "braided" structures, stretched filaments, and double layers. In this paper

[1] Now at Swedish Institute of Space Physics, Kiruna, Sweden.

Paper number 97RS00088.
0048-6604/97/97RS-00088$11.00

we will collectively refer to these patterns as Kelvin-Helmholtz billows, or KH billows for short. The KH billows form perpendicular to the vertical wind shear and travel with the mean horizontal wind. Beautiful examples of KH billows in the atmospheric boundary layer have been documented by *Eaton et al.* [1995].

In the past, radar investigations of KHI have been performed using a host of techniques. High-powered meteorological radars have provided two-dimensional images of KH billows occurring up to the tropopause [e.g., *Browning*, 1971; *Reed and Hardy*, 1972]. These observations, however, are limited in range resolution. High-powered radars using vertically and near vertically oriented radar beams have also been used, providing the vertical structure of large-amplitude KH billows [e.g., *VanZandt et al.*, 1979; *Klostermeyer and Rüster*, 1980]. These measurements are also limited in range resolution. On the other hand, frequency-modulated continuous wave (FM-CW) radars have been employed to obtain observations of KHI having excellent range resolution [e.g., *Gossard et al.*, 1970; *Eaton et al.*, 1995]. Here the limitation is that they are only capable of making observations in the planetary boundary layer.

In this paper we investigate the possibility of studying KHI using yet another radar technique, frequency domain interferometry (FDI). When employing the FDI technique, the radar transmits and receives two or more different frequencies in an alternating sequence. Cross-correlation or cross-spectral analysis is then conducted on two of the resulting complex radar time series. If the energy has been primarily scattered from a single atmospheric layer that is thin in comparison with the vertical extent of the sampling pulse, then the two radar time series will be highly correlated. Furthermore, the magnitude and phase angle of the correlation coefficient can be used to provide estimates of a layer's width and location, respectively. For further discussion on the mathematical development of the FDI technique, see, for example, *Franke* [1990] and *Chu and Chen* [1995].

We present here results from an experiment conducted on March 10 through 13, 1995, using the sounding system (SOUSY) VHF radar while operating in an FDI mode. Using FDI, it is possible to trace the vertical motion of a layer, even when its displacement is less than the conventional radar range resolution. During the latter half of the observations, an upper level jet passed over the radar, producing horizontal winds in excess of 60 m s^{-1}. Structures resembling KH billows were found in the shear regions both above and below the core of the jet stream. In this paper we will begin by describing the radar and the mode in which it was operating. Then we discuss methods used to analyze the radar data and present an overview of the data set. Finally, we examine one of the trains of KH billows in detail.

Experimental Description

The SOUSY VHF radar is located in the German Harz Mountains (51.66°N, 10.49°E) and operates at a nominal frequency of 53.5 MHz. It has a peak transmitted power of 600 kW with a duty cycle of 4% and uses a phased array antenna consisting of 196 Yagi elements [*Czechowsky et al.*, 1984]. The radar has recently been modified to facilitate FDI observations using multiple operating frequencies [*Chilson and Schmidt*, 1996]. For the measurements presented in this paper, the radar transmitted and received pulses having frequencies of 53.25 and 53.75 MHz on an alternating basis. The sampling range consisted of two overlapping regions having different pulse coding schemes. In the range of 1.6–7.3 km, single pulses were used, and in the range of 3.7–15.4 km, an 8-bit complementary code was used [*Schmidt et al.*, 1979]. For both regions a range resolution of 300 m was chosen.

Observations were conducted using the radar during the period of March 10–13, 1995. The experiment was designed to detect atmospheric waves having small periods and amplitudes. Consequently, the radar was primarily operated in a vertical mode, with the exception of 11-min interruptions every 66 min to allow Doppler beam swinging (DBS) wind measurements. In the DBS mode, the radar beam was directed vertically and at 7° off vertical toward the north, east, south, and west. The hourly DBS observations consisted of 10 cycles through the five beam orientations. For each beam direction in both the vertical and DBS modes, the received signal was recorded as 128 complex time series points for the two alternating frequencies, which is a total of 64 pulses at 53.25 MHz and 64 pulses at 53.75 MHz. The 128 time series points were then written to a storage disk as a single beam record. Each time series point was calculated from 50 coherent integrations, resulting in a sampling period of approximately 100 ms. The resulting dwell time for each beam direction was 12.8 s. The pulse scheme was the same as that described by *Chilson and Schmidt* [1996].

The radar data collected on March 10–13 have

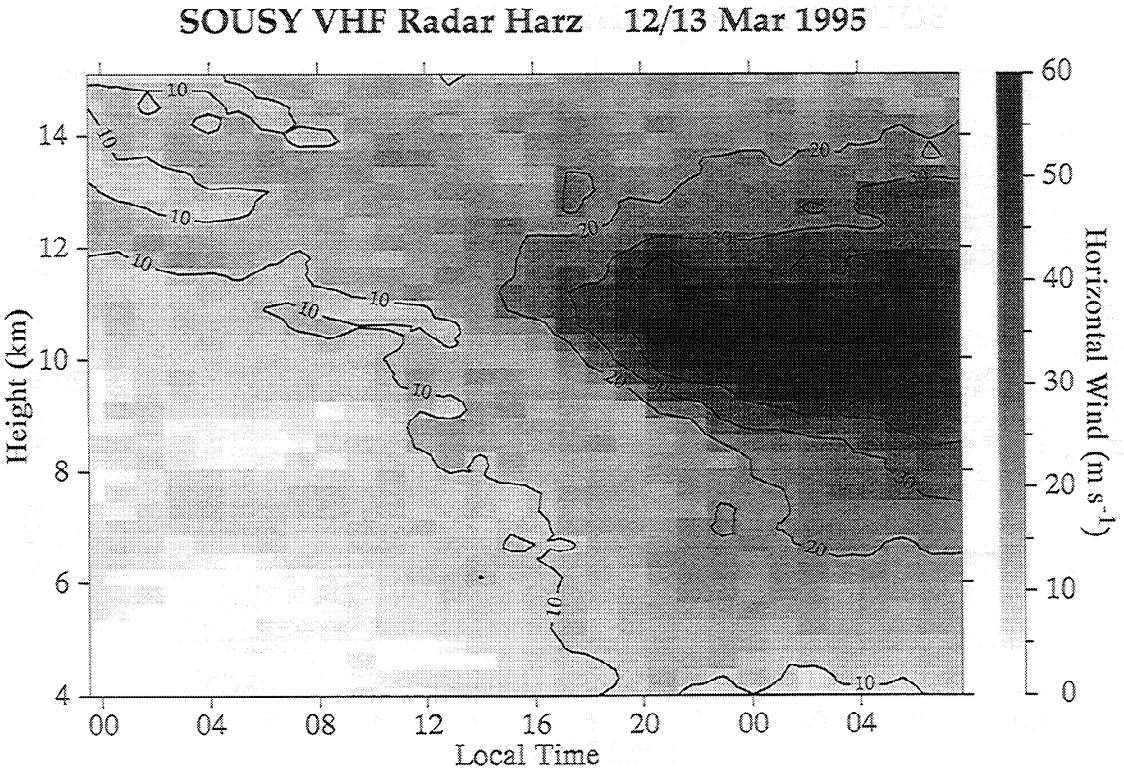

Figure 1. Contour plot of the horizontal wind observed in association with the onset of a jet stream on March 12, 1995, at approximately 1600 LT and at an altitude of 10.5 km. Contour lines have been drawn showing the 10, 20, 30, 40, 50, and 60 m s^{-1} velocity levels.

been divided into two separate time intervals for analysis. During the initial half of the observations the radar site was in a system of high pressure, giving rise to statically stable atmospheric conditions. In the second half of the observations an upper level jet passed over the radar, producing horizontal winds in excess of 60 m s^{-1} at altitudes of about 10 km. The presence of the jet can be seen in the radar-derived horizontal wind velocities for roughly 16 hours. Unfortunately, a hardware problem disabled the radar before the jet stream had a chance to completely pass over the site.

Data Analysis and Overview

Doppler Beam Swinging Processing

We begin our analysis by examining the data recorded while the radar operated in the DBS mode. As mentioned earlier, 10 sets of five-beam DBS cycles were performed every 66 min, corresponding to a total of 10 min and 40 s of observation time. For each beam the complex time series data were separated in frequency, and Doppler power spectra were calculated using the fast Fourier transform method, yielding two independent autospectra. Taking the magnitudes of the autospectra, averages were calculated for a given beam direction over the entire DBS cycle. That is, five Doppler spectra were found, one for each beam orientation and each consisting of 20 spectral averages. Finally, the radial velocities were found for each Doppler spectrum by calculating the first moment after having removed the noise. All five radial velocities were used in a least squares–fit analysis to generate estimates of the u, v, and w components of the wind for each height increment [*Rüster*, 1994].

A plot of the hourly sampled horizontal winds measured from March 12–13 is shown in Figure 1 as a contour plot in altitude and time. The entrance of the jet stream began at roughly 1600 LT on March 12 and reached a maximum horizontal wind speed of roughly 65 m s^{-1} around 0000 LT. The core of the jet was located at an altitude between 10 and 10.5 km.

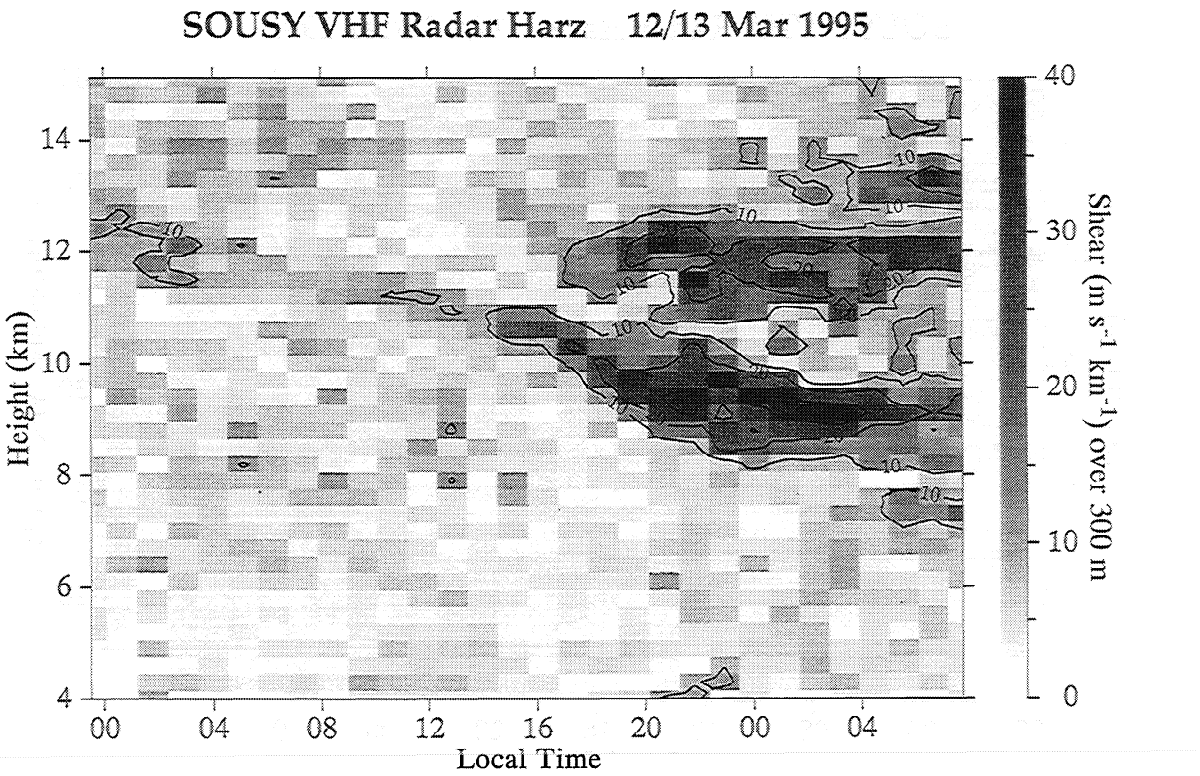

Figure 2. Wind shear calculated from the data shown in Figure 1 using equation (1). The shear was calculated over a height interval of 300 m and has been expressed in m s^{-1} km^{-1}. Shown are the 10, 20, and 30 m s^{-1} km^{-1} contour lines.

The horizontal wind of the jet stream appears to have reached a maximum and was exiting when a radar failure occurred at 0847 LT.

Since KHI are to be expected in regions characteristic of large vertical shears in the horizontal wind, we next examine this quantity. The total shear has been calculated using

$$S_z = \sqrt{\left(\frac{\Delta u}{\Delta z}\right)^2 + \left(\frac{\Delta v}{\Delta z}\right)^2}, \qquad (1)$$

where Δu and Δv are the changes in the zonal and meridional components of the wind across the sampling volume, respectively, and Δz is the range resolution of the radar, here 300 m. We have calculated the shear using the data shown in Figure 1, and the results are given in Figure 2, again in a time-height contour plot. Note that the units of m s^{-1} km^{-1} have been chosen to express the magnitude of the shear.

As expected, the regions in which the shear is the strongest lie above and below the axis of the jet stream. In the next section we show that these shear zones correspond to the location of atmospheric layers. The largest values of S_z are located below the jet stream. In particular, a persistent shear region can be seen between 0000 and 0400 LT at a height of 9 km. KH billows have been detected in the radar data both above and below the jet stream, and in the next section we present an example of one such event.

Frequency Domain Interferometry Processing

We next consider the observations from an FDI perspective. For this purpose we only use those data from the vertical mode. In our analysis we have adapted the procedure of *Franke* [1990] for estimating the location and width of a scattering layer as discussed by *Chilson and Schmidt* [1996]. To begin the calculation of a scattering layer's altitude and width, we found the correlation coefficient S_{12} from the time series data for the two carrier frequencies as given by

$$S_{12} = \frac{\langle V_1 V_2^* \rangle}{\sqrt{\langle |V_1|^2 \rangle \langle |V_2|^2 \rangle}}. \qquad (2)$$

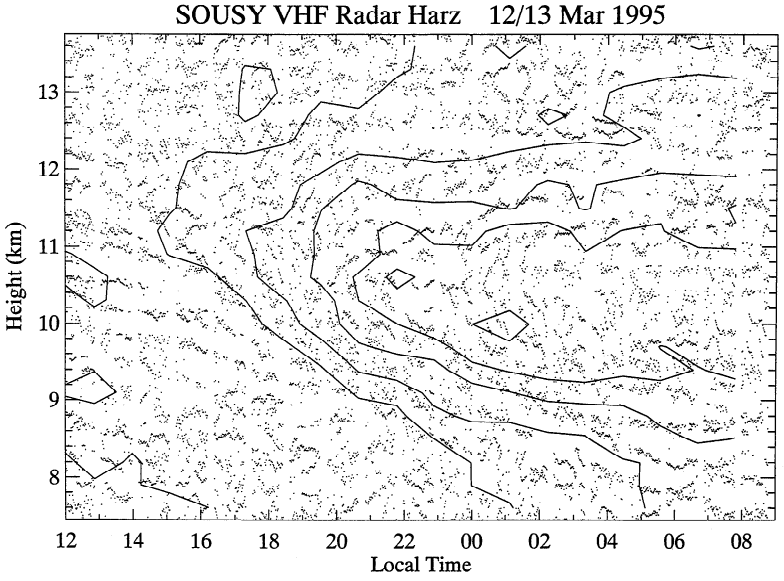

Figure 3. A depiction of the location of scattering centers as retrieved using the frequency domain interferometry technique. Also shown are contour lines of the horizontal wind magnitude. As in Figure 1, the 10, 20, 30, 40, 50, and 60 m s^{-1} velocity levels are given.

Here V_n represents the voltage samples for the two frequencies, the asterisk denotes a complex conjugate, and angle brackets indicate an ensemble average over a collection of time series points.

If a single "thin" scattering layer is present within a sampling volume, the amplitude and phase of S_{12} can be used to provide an estimate of the location and width of the layer [*Franke*, 1990; *Kudeki and Stitt*, 1990]. Using equations (3) and (4) from *Chilson and Schmidt* [1996], we calculated the location of a scattering layer z_l and its thickness σ_l. These equations are derived assuming a turbulent layer weighted by a Gaussian function given by $\exp[-(z - z_l)^2/2\sigma_l^2]$. An error in the estimate of the layer thickness will result for the case of non-Gaussian turbulent layers or sharp nonturbulent gradients in the atmospheric refractive index [*Chu and Chen*, 1995]. We have therefore chosen to use the coherence $|S_{12}|$, as opposed to σ_l, as a parameterization of the width of a layer. Note that the value of z_l remains relatively unaffected for the different types of layers. For a more thorough description of the application of the FDI technique to data from the SOUSY VHF radar, see *Chilson and Schmidt* [1996].

It is important to mention that even if no well-defined layer exists within the radar sampling volume, the FDI-derived value of z_l can still be a useful quantity if it is interpreted as the altitude from which the majority of the backscattered signal originates. That is, z_l locates the height of the center of the maximum backscattering density. Therefore we will also at times refer to z_l as the height of the scattering center for each range bin. We should also point out that if two or more nonoverlapping horizontally distributed scattering centers are located within a radar sampling volume, then the value of z_l gives a weighted average of their locations.

To reproduce the large-scale structures in the atmosphere in connection with the jet stream, we have processed the FDI data using five consecutive vertical beam records, or 67 s. A portion of the results are given in Figure 3. Be aware that the time and height axes have been chosen differently than those shown in Figures 1 and 2. The figure represents the FDI-estimated location of the scattering centers found within each 300-m range bin. Within each height interval, a 67-s-long line segment has been drawn indicating the value of z_l. No information regarding the scattering center's width has been included in Figure 3. Also shown in Figure 3 are contour lines of the horizontal wind magnitude. These are the same as have been shown in Figure 1. Additional examples of large-scale atmospheric structures observed using FDI are given by *Kilburn et al.* [1995] and *Chilson and Schmidt* [1996].

A striking feature of Figure 3 is the layered struc-

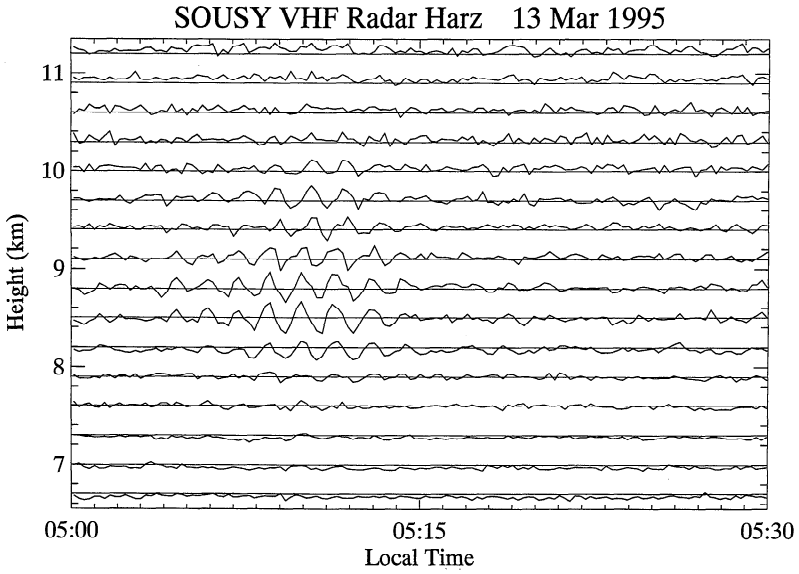

Figure 4. Unfiltered radial velocities measured while the radar beam was oriented vertically. The large-amplitude oscillations mark the occurrence of a Kelvin-Helmholtz instability (KHI). The velocities have been scaled such that 1 m s^{-1} corresponds to 100 m.

tures seen in the immediate vicinity of the jet. Here the layers slope upward above the jet and downward below it, producing an envelope that coincides well with the regions of strongest shear. Note the region located between 10 and 12 km from 2000 to 0200 LT, where a scattering layer is particularly evident. As can be seen in Figure 2, the layer coincides with a region of large shear. Although not presented in this paper, we have found evidence of KHI in the vicinity of several of the layers shown in Figure 3. In the next section we will discuss a KHI that occurred on March 13 around 0515 LT in the height range of 8–10 km.

Detection of Kelvin-Helmholtz Instability and Kelvin-Helmholtz Billows

In this section we discuss a portion of the data in which evidence of KHI and KH billows can be seen. The time and location of the KH billows correspond to the regions of strong vertical wind shear mentioned earlier in the paper. The case to be presented coincides with the shear region below the jet axis seen in Figure 2 located at a height between 9 and 10 km. In the analysis we first present the KHI as seen in the radial Doppler velocities v_r between 8 and 10 km. Then we make a comparative analysis of the signal-to-noise ratio (SNR), the radial Doppler velocity v_r, the coherence $|S_{12}|$ as calculated using (2), and the FDI-derived height of a scattering center z_l. Features in the time histories of these quantities indicate a train of KH billows. All of the data were obtained while the radar operated in the vertical mode, and each value was calculated from a single beam record (13 s).

Kelvin-Helmholtz Instability

We consider a region of the radar data between 0500 and 0530 LT for the altitude range centered at about 9 km. This time and height interval has been chosen on account of the onset and decay of large oscillations in radial Doppler velocities, which for the vertical beam represent w. The oscillations can be seen in Figure 4, which shows time histories of the unfiltered values of w. The oscillations begin developing around 0505 LT and last for approximately 10 min. During this time the amplitude of the billows grew continuously up to a value of 1.6 m s^{-1} at around 0510 LT, and then decayed. The oscillations were evident over a height range of about 2 km and within this range have a constant observed period of 90 s. An interesting feature of the oscillations occurs between 9.1 and 9.4 km, where their phase undergoes an abrupt shift of roughly 90°. Similar wave events have been observed by *VanZandt et al.* [1979], *Klostermeyer and Rüster* [1980, 1981], and *Rüster and*

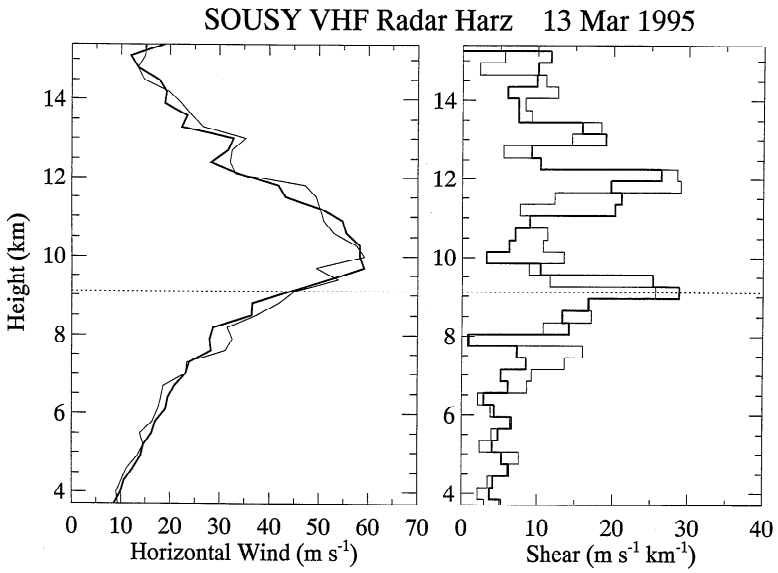

Figure 5. Height profiles of the horizontal wind and the vertical wind shear. The profiles were measured at 0427 LT (bold lines) and 0534 LT (light lines). The horizontal dashed lines mark the 9.1-km height.

Klostermeyer [1983] and are indicative of the presence of a KHI.

To appreciate the vertical structure of the atmosphere during the time of the KHI shown in Figure 4, it is necessary to examine the horizontal wind and its vertical shear on a smaller timescale than used in Figures 1 and 2. We have examined the height profiles of the horizontal wind and its vertical shear S_z calculated from the DBS data obtained just before and after the occurrence of KHI. The exact start times of the DBS data–collecting cycles were 0427 and 0534 LT. These profiles of the horizontal wind and the shear are shown in Figure 5. Both profiles of S_z exhibit local peaks at a height of 9.1 km. The magnitudes of the peaks are 29 and 26 m s^{-1} km^{-1} before and after the KHI, respectively. Note that the S_z-profile peak measured before the KHI reveals a region of vertical shear approximately 600 m thick. The thickness of the layer will be shown later to play a role in the generation of KH billows.

Unfortunately, we have no measurements of the Brunt-Väisälä period T_{BV} corresponding to the time and location of the KHI. Therefore we cannot calculate the Richardson number *Ri*. However, we can obtain an approximation of *Ri* by using data from routine radiosonde launches. The nearest meteorological station to the SOUSY VHF radar is Hannover-Langenhagen, which is located 110 km to the northwest. Radiosonde measurements made on March 13 at 0000 UT (0100 LT) indicate the value of T_{BV} to be 9 min [*Deutscher Wetterdienst*, 1995]. Using this Brunt-Väisälä period, together with the S_z measurements before and after the KHI, we find *Ri* values of 0.17 and 0.21, respectively, which are below the critical value of 0.25.

Kelvin-Helmholtz Billows

The oscillations shown in Figure 4, along with the height profiles of the vertical shear, provide strong evidence that a KHI occurred between 0500 and 0515 LT near an altitude of 9.1 km. Note that the altitude of 9.1 km also corresponds to the expected altitude of the critical layer in connection with the KHI. We now look for evidence of KH billows within the time histories of SNR, v_r, $|S_{12}|$, and z_l for the height of 9.1 km. These four quantities are plotted in Figure 6. In all four traces, the plus symbols indicate the values as calculated from the data within a single beam record. The 95% significance level for the coherence as calculated using equations (5) and (6) of *Chilson and Schmidt* [1996] has been shown as a horizontal dashed line. In reality, the significance level varies from point to point, but these fluctuations are small for the example given. During the time of the largest velocity oscillations, that is, during the time of the KHI, most

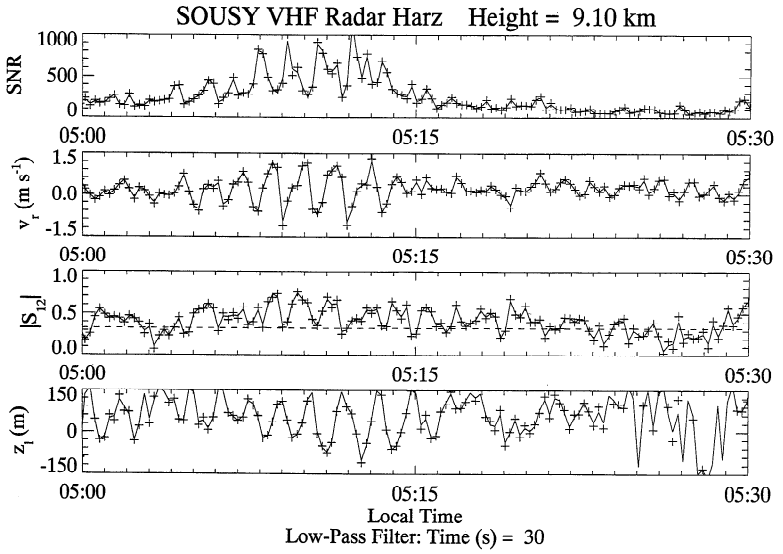

Figure 6. Time histories of four quantities measured with the radar showing evidence of KH billows below the axis of the jet stream. Plotted are the signal-to-noise ratio (SNR), the radial Doppler velocity v_r, the coherence $|S_{12}|$, and the scattering center height z_l for March 13, 1995. The symbols show the actual calculated values, and the solid line indicates the values after being low-pass filtered.

of the FDI coherence values are statistically significant.

To remove high-frequency oscillations, the data have been filtered using a nonrecursive digital filter. The results are shown in Figure 6 as the solid line. Although this is a filter in the frequency domain, the cut-off value will be discussed in the text in terms of its corresponding period. For the data shown in Figure 6, a 30-s low-pass filter was used. That is, we attempted to remove all frequencies of 3.33×10^{-2} Hz and higher. Note that one must be careful when applying a filter function to the values of z_l. For example, filtering would not be possible if more than one layer were to pass through a sampling range during the time the filter was being applied. For the data shown in Figure 6, the layer is contained within the bounds of the sampling range for at least the first 25 min.

Figure 6 shows that oscillations associated with the KHI are not only present in the radial velocity but are also evident in the radar signal power, the coherence, and the layer position as well. Furthermore, all of the oscillations, although not coherent in phase, have a local period of approximately 90 s. We would like to especially emphasize the bottom two panels of the figure, which express information about the structure of the billows. The FDI technique has made it possible to track the altitude of the KH billow with a vertical accuracy of a few tens of meters and at a temporal resolution of 13 s, corresponding to an in-stream horizontal resolution of a few hundreds of meters. Furthermore, the KH billow is found to have amplitudes of roughly 200 m, less than the conventional range resolution of the radar. In addition, the coherence $|S_{12}|$ gives a qualitative estimate of the layer's thickness, with large values corresponding to thin layers or scattering centers. We know of no other radar method capable of obtaining such measurements at an altitude of 9 km.

On the basis of various combinations of the radar-derived quantities, we can now attempt to calculate some properties of the KHI. Utilizing the property of KHI that they are advected with the background wind, the observed oscillation period was used to calculate the horizontal wavelength of the KH billow. At the time and height of the instability, the horizontal wind had a magnitude of 45 m s^{-1}, leading to a wavelength λ_x of 4.0 km, assuming that the angle between the wind vector and the vector of the vertical wind shear is negligible (see discussion below). The value of λ_x falls within the range of wavelengths observed by *Browning* [1971]. When dealing with KHI in a shear zone, it is common to invoke the equation

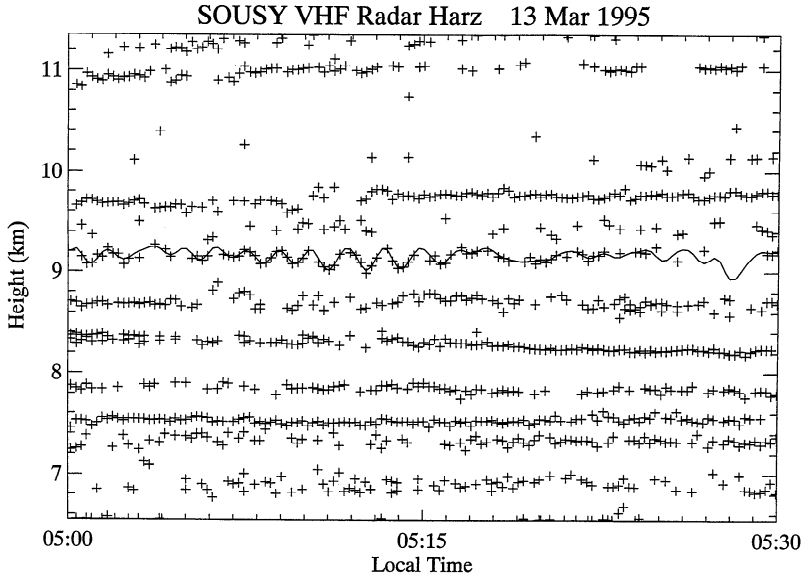

Figure 7. Time-height plot of z_l similar to that shown in Figure 3. Each point in the figure was calculated from 13 s of data and corresponds to a coherence greater than 0.33. Also shown are the low-pass-filtered values of z_l for the height of 9.1 km.

$$\lambda_x = 7.5\Delta Z, \tag{3}$$

where ΔZ is the thickness of a sheared layer [e.g., *Browning*, 1971; *Fritts and Rastogi*, 1985]. Here λ_x is the most unstable, and hence fastest growing, wavelength within a region of KHI. Taking the observed value of 600 m as the vertical extent of the shear zone, (3) predicts the fast growing billow to have a wavelength of 4.5 km, which is in good agreement with the inferred value of 4 km. Note that we must be cautious when interpreting this result, since the range resolution of the wind shear measurements was 300 m. Furthermore, the KH billows are aligned in the direction of the background shear, which can be different from that of the background wind. The two are approximately parallel above and below the KH billows, but at a height of 9.1 km their angular directions differ by 23° and 38° before and after the KHI, respectively. Finally, we consider the ratio of the crest-to-trough amplitude to the wavelength for the KH billow. Examining the FDI-estimated trace of the layer height shown in the bottom panel of Figure 6, we find that the crest-to-trough amplitude reached a maximum value of 220–230 m shortly before 0515 LT. Therefore, taking $\lambda_x = 4.0$ km, the ratio is given by 0.06. The ratios reported by *Browning* [1971] ranged from 0.1 to 0.5 with a mean of 0.25.

It is not clear from Figure 6 whether the values of z_l overspread into the neighboring range intervals. This would result in an underestimation of the measured crest-to-trough amplitude. Therefore we show in Figure 7 a time-height plot of the estimated positions of the scattering centers near the KHI. The region that has been chosen is the same as that shown in Figure 4. Each value of z_l in the figure was calculated from 13 s of data and corresponds to a coherence greater than 0.33. On the basis of data for the height of 9.1 km, this relates to a 95% significance. The solid line shows the low-pass-filtered data for z_l, where oscillations having periods less than 60 s have been suppressed. The KH billows at a height of 9.1 km are confined to within a single range interval. Therefore the amplitude estimate of 220–230 m is probably an accurate indication of the crest-to-trough vertical extent of the KH billow.

To investigate the amplitude and phase relationships between the quantities shown in Figure 6, we have applied a 60-s low-pass filter to the data. The resulting traces are given in Figure 8. The presence of a 90-s wave oscillation is now especially apparent in all of the time histories. In addition, we see that there are fairly constant phase relationships between the quantities during the time of the KHI. When com-

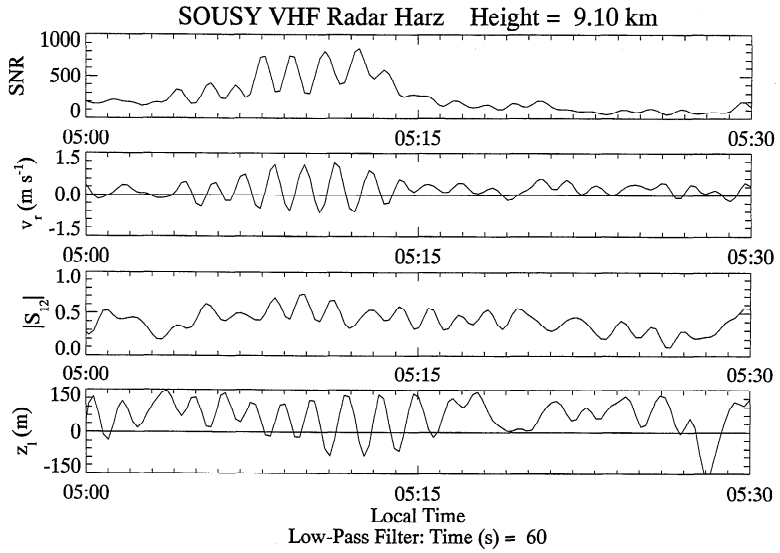

Figure 8. The same quantities as shown in Figure 6 after being low-pass filtered. Oscillations having periods less than 60 s have been suppressed.

paring the traces, it is important to be reminded of the phase jump that occurs in the trace of v_r near the 9.1 km altitude level.

The following observations can be made based on the data shown in Figure 8. Between 0506 and 0514 LT, five consecutive maxima in the SNR are found to coincide with increases in the radial velocity, increases in the coherence, and minima in the layer altitude. Conversely, a minimum in the SNR coincides with a decrease in the radial velocities, a decrease in coherence, and a maximum in layer position. Oscillations in the coherence persisted past 0515 LT, even after signs of the KHI have vanished. It is also interesting to note that the phase of layer position z_l leads the phase of the radial (vertical) velocity by 90°. This is consistent with the assumption that the oscillations in the vertical velocity reflect the vertical motions of the layer.

We have compared our data with those of *Klostermeyer and Rüster* [1981], who reported VHF radar observations during a similar KHI event. They have conducted a detailed investigation of the relationship between radial velocity observations and sudden bursts in the radar signal power measured within a KHI. From their data, *Klostermeyer and Rüster* [1981, p. 6634] found that "the power bursts coincide with increasing radial velocities after the amplitude of the KHI has exceeded a certain threshold." This feature is clearly seen in the traces of SNR and v_r shown in Figure 8. For comparison, refer to Figure 8 of *Klostermeyer and Rüster* [1981]. Note that they have plotted S/S_0, which is a normalized power value, where S and S_0 are the original and low-pass-filtered power data, respectively. Furthermore, the radial velocities of *Klostermeyer and Rüster* [1981] were measured with an oblique beam (12.5° off vertical), whereas our radial velocities were measured with a vertical beam. The fluctuations in both most likely reflect the vertical motions of the billows. Although slightly different in presentation, both S/S_0 and the low-pass-filtered value of SNR depict changes in the radar signal power. Taking this into consideration, the relationship between the radar signal power and the radial velocity shown in Figure 8 of *Klostermeyer and Rüster* [1981] and in our Figures 6 and 8 are quite similar.

One of the open questions asked by *Klostermeyer and Rüster* [1981, p. 6636] was "whether the KHI-associated power bursts are mainly produced by scattering from small-scale irregularities or by partial reflections from large-scale stratifications of the refractive index." If the power bursts were associated with small-scale irregularities, then a peak in the SNR should coincide with a minimum in the coherence. Likewise, if the bursts were attributed to partial reflections resulting from large-scale stratifications, then a peak in the SNR should correspond with a maximum in the coherence. Our observations show the SNR peak occurred shortly after a minimum in

the coherence. This indicates that the power bursts were related to a phase in the KH billow in which it becomes hydrostatically unstable, consistent with the observations of *VanZandt et al.* [1979].

Discussion

In this paper we have examined radar data collected between March 12–13, 1995, during the passage of an upper level jet. On a large scale, FDI has reproduced layered structures in the vicinity of the jet stream that coincide well with regions of vertical shear found in the horizontal wind. These layers were distributed over an altitude range of several kilometers and persisted at times over many hours. Conversely, FDI can also provide information on small-scale processes, as illustrated by the observations of a train of KH billows with vertical and temporal resolutions of a few tens of meters and 13 s, respectively. The observed KH billow that occurred below the axis of the jet stream had a peak-to-trough amplitude of up to 230 m, which is less than the conventional radar range resolution of 300 m used during the experiment. Using FDI, we were able to track the location of the billow's scattering over six or more full periods.

Some of the observed or inferred characteristics of the KHI and the resulting KH billow are listed here. The KHI was observed for approximately 10 min and was located near an altitude of 9.1 km. The horizontal wind speed at this height was 45 m s^{-1}, suggesting that the horizontal extent of the KHI was about 27 km. From the observed period of the KH billow, we calculated the wavelength to be 4.0 km. On the basis of a calculation using the depth of the shear zone in which the KHI occurred, we found the expected wavelength to be 4.5 km. Similar to the observations reported by *Klostermeyer and Rüster* [1981], we detected peaks in the radar signal power within the KHI that formed during the growth phase of the radial velocities. The signal power peaks also coincided with an increase in the FDI coherence and a decrease in the layer altitude; however, interpretation of these results requires further investigation.

Acknowledgments. We are grateful to J. Klostermeyer for his helpful comments while preparing this paper. We also appreciate the kind assistance provided by the members of the SOUSY research group. One of us (P.B.C.) was supported by a stipend from the Max-Planck-Gesellschaft zur Förderung der Wissenschaften.

References

Atlas, D., J. I. Metcalf, J. H. Richter, and E. E. Gossard, The birth of "CAT" and microscale turbulence, *J. Atmos. Sci.*, *27*, 903–913, 1970.

Browning, K. A., Structure of the atmosphere in the vicinity of large-amplitude Kelvin-Helmholtz billows, *Q. J. R. Meteorol. Soc.*, *97*, 283–299, 1971.

Browning, K. A., and C. D. Watkins, Observations of clear air turbulence by high power radar, *Nature*, *227*, 260–263, 1970.

Chilson, P. B., and G. Schmidt, Implementaion of frequency domain interferometry at the SOUSY VHF radar: First results, *Radio Sci.*, *31*, 263–272, 1996.

Chu, Y. H., and T. N. Chen, A theoretical study of two-frequency coherence of MST radar returns, *Radio Sci.*, *30*, 1803–1815, 1995.

Czechowsky, P., G. Schmidt, and R. Rüster, The mobile SOUSY Doppler radar: Technical design and first results, *Radio Sci.*, *19*, 441–450, 1984.

Deutscher Wetterdienst, *Europäishcer Wetterbericht*, Amtsblatt des Deutschen Wetterdienstes, *20*, Offenbach, Germany, 1995.

Eaton, F. D., S. A. McLaughlin, and J. R. Hines, A new frequency-modulated continuous wave radar for studying planetary boundary layer morphology, *Radio Sci.*, *30*, 75–88, 1995.

Franke, S. J., Pulse compression and frequency domain interferometry with a frequency-hopped MST radar, *Radio Sci.*, *25*, 565–574, 1990.

Fritts, D. C., and P. K. Rastogi, Convective and dynamical instabilities due to gravity wave motions in the lower and middle atmosphere: Theory and observations, *Radio Sci.*, *20*, 1247–1277, 1985.

Gage, K. S., Radar observations of the free atmosphere: Structure and dynamics, in *Radar in Meteorology*, edited by D. Atlas, pp. 534–565, Am. Meteorol. Soc., Boston, Mass., 1990.

Gossard, E. E., Radar research on the atmospheric boundary layer, in *Radar in Meteorology*, edited by D. Atlas, pp. 477–527, Am. Meteorol. Soc., Boston, Mass., 1990.

Gossard, E. E., and W. H. Hooke, *Waves in the Atmosphere*, Elsevier, New York, 1975.

Gossard, E. E., J. H. Richter, and D. Atlas, Internal waves in the atmosphere from high-resolution radar measurements, *J. Geophys. Res.*, *75*, 3523–3536, 1970.

Hicks, J. J., and J. K. Angell, Radar observations of breaking gravitational waves in the visually clear atmosphere, *J. Appl. Meteorol.*, *7*, 114–121, 1968.

Kilburn, C., S. Fukao, and M. Yamamoto, Extended period frequency domain interferometry observations at stratospheric and tropospheric heights, *Radio Sci.*, *30*, 1099–1109, 1995.

Klostermeyer, J., and R. Rüster, Radar observations and model computation of a jet stream–generated Kelvin-

Helmholtz instability, *J. Geophys. Res.*, *85*, 2841–2846, 1980.

Klostermeyer, J., and R. Rüster, Further study of a jet stream–generated Kelvin-Helmholtz instability, *J. Geophys. Res.*, *86*, 6631–6637, 1981.

Kudeki, E., and R. Stitt, Frequency domain interferometry studies of mesospheric layers at Jicamarca, *Radio Sci.*, *25*, 575–590, 1990.

Reed, R. J., and K. R. Hardy, A case study of persistent, clear air turbulence in an upper-level frontal zone, *J. Appl. Meteorol.*, *11*, 541–549, 1972.

Rüster, R., Analysis and interpretation of VHF-radar data, *Ann. Geophys.*, *12*, 725–732, 1994.

Rüster, R., and J. Klostermeyer, VHF radar observations of a Kelvin-Helmholtz instability in a subtropical jet stream, *Geophys. Astrophys. Fluid Dyn.*, *26*, 107–116, 1983.

Schmidt, G., R. Rüster, and P. Czechowsky, Complimentary code and digital filtering for detection of weak VHF radar signals from the mesosphere, *IEEE Trans. Geosci. Electron.*, *GE-17*, 154–161, 1979.

VanZandt, T. E., J. L. Green, and W. L. Clark, Buoyancy waves in the troposphere: Doppler radar observations and a theoretical model, *Geophys. Res. Lett.*, *6*, 429–432, 1979.

P. Chilson, Swedish Institute of Space Physics, Box 812, S-981 28 Kiruna, Sweden. (e-mail: phil@irf.se)

A. Muschinski, Institut für Meteorologie und Klimatologie der Universität Hannover, Herrenhäuser Str. 2, D-30419 Hannover, Germany.

G. Schmidt, Max-Planck-Institut für Aeronomie, P.O. Box 20, D-37189 Katlenburg-Lindau, Germany.

(Received July 11, 1996; revised December 4, 1996; accepted January 10, 1997.)